JOM, Vol. 66, No. 10, 2014
DOI: 10.1007/s11837-014-0953-8

Phase Selection in High-Entropy Alloys: From Nonequilibrium to Equilibrium

ZHIJUN WANG,[1,2] SHENG GUO,[3] and C.T. LIU[1,4]

1.—Center of Advanced Structural Materials, Department of Mechanical and Biomedical Engineering, College of Science and Engineering, City University of Hong Kong, Kowloon, Hong Kong, People's Republic of China. 2.—State Key Laboratory of Solidification Processing, Northwestern Polytechnical University, Xi'an 710072, People's Republic of China. 3.—Surface and Microstructure Engineering Group, Department of Materials and Manufacturing Technology, Chalmers University of Technology, 412 96 Göteborg, Sweden. 4.—e-mail: chainliu@cityu.edu.hk

High-entropy alloys (HEAs) have been investigated considerably in the last decade. The phase selection in HEAs has attracted much attention recently, especially on forming of the solid solutions. Up to now, phase diagrams of most HEAs are still not well developed, and the empirical phase selection rules play an important role in HEAs area. In this brief review, the physical factors controlling the phase stability in HEAs are discussed, and the phase selection rules are identified. Different from previous results, the rules on equilibrium phase selection within a certain temperature range are carefully reviewed and presented in this article.

INTRODUCTION

High-entropy alloys (HEAs) constitute a class of novel, multicomponent alloys consisting of more than four elements with equal or nearly equal molar fractions.[1–6] The high configurational entropy in HEAs is considered to suppress the formation of intermetallic compound and stabilize simple solid solutions. HEAs have drawn much attention recently because of their remarkable mechanical properties, including high hardness, good wear and corrosion resistance, and high-temperature softening resistance. As a new class of multicomponent alloys, HEAs are complex in the phase selection because of their high configurational entropy, sluggish diffusion, severe lattice distortion, and cocktail effects.[5,6] In principle, thousands of element assemblies for HEAs can exist based on the Periodic Table; however, candidate alloys for potential engineering applications have to be carefully screened, with phase selection as the first critical step to search for HEAs with desirable properties.

Although a significant progress has been made on the metallurgical and physical understanding of HEAs, the phase diagram as a fundamental issue is not fully solved. Preliminary work has been done on phase diagrams for a very limited number of HEAs, and it is still challenging to precisely determine their phase diagram because of the multiprincipal elements and sluggish kinetics.[7–9] HEAs can exist as solid solutions, intermetallic compound, amorphous alloys, or a mixture of these phases. Based on the experimental results obtained so far, the phase selection in HEAs is related to several characteristic parameters. From the experimental results and thermodynamic analyses, several simple rules useful for the phase selection in HEAs have been proposed in recent years.[10–14]

On the one hand, the previous phase selections were mainly analyzed for experiments from as-cast samples prepared from the rapid solidification occurring in copper molds with small sizes. Thus, the phase selection obtained previously is essentially associated with the alloying states at high temperatures. On the other hand, some HEAs with attractive properties have been identified for structural applications at high temperatures, such as structural materials in power plants.[15,16] This can certainly justify the merit of previously established phase selection rules. However, in principle, the phase stability in the equilibrium state should be understood prior to any possible structural applications of HEAs. Thus, the determination and prediction of the equilibrium phases as a function of certain temperature in HEAs are of vital importance. In this review, the phase selection rules

(Published online April 24, 2014)

obtained so far from both theoretical analyses and experimental studies will be carefully reviewed and verified. Also, we will discuss the equilibrium phase selection based on a plenty of heat-treatment experiments within a certain temperature range.

PHYSICAL PARAMETERS FOR THE PHASE SELECTION

In thermodynamics, the phase transformation depends on the Gibbs free energy difference,

$$\Delta G_{\text{mix}} = \Delta H_{\text{mix}} - T\Delta S_{\text{mix}} \quad (1)$$

where ΔG_{mix} is the change in the Gibbs free energy that arises from the mixing of individual constituents, ΔH_{mix} and ΔS_{mix} are the changes in enthalpy and entropy, respectively. Solid solutions have a relatively larger configurational entropy compared with intermetallic compounds. Therefore, the solid-solution phase is expected to be more stable at high temperatures because of the temperature-dependent term of $-T\Delta S_{\text{mix}}$. However, the mixing enthalpy ΔH_{mix} in some HEAs is quite negative, and as a result, the forming of intermetallic compounds cannot be totally avoided. Accordingly, the mixing enthalpy is another important characteristic parameter affecting the phase selection in HEAs. In a random solid solution, the mixing enthalpy is usually defined as[10,13]

$$\Delta H_{\text{mix}} = \sum_{i,j=1,i\neq j}^{n} \alpha_{ij} c_i c_j \quad (2)$$

where $\alpha_{ij} = 4\Delta H_{AB}^{\text{mix}}$, $\Delta H_{AB}^{\text{mix}}$ is the mixing enthalpy for the binary AB alloy, and $c_i(c_j)$ is the molar concentration of the ith(jth) atom.

From the strain energy consideration, the geometrical factor, atomic radius of alloying elements, also greatly influences the solid-solution stability and hence the phase stability. In Hume-Rothery rules,[17] the atomic-size difference between the solvent and solute could not exceed 15% in binary solid solutions. In HEAs, there are no specific solvent and solute elements. The dispersion of atomic sizes is thus selected to describe the solid-solution stability. The parameter related to the atomic-size difference δ is defined as[10,13]

$$\delta = \sqrt{\sum_i^n c_i(1 - r_i/\bar{r})^2}, \ \bar{r} = \sum_i^n c_i r_i \quad (3)$$

where r_i is the atomic radius of the ith atom.

Both face-centered cubic (fcc) and body-centered cubic (bcc) solid-solution structures can form in HEAs. In conventional multicomponent alloys, the structure selection is normally considered from the effects of the additional elements (solute atoms) on the structure of the principal element (solvent atom). In HEAs, there are several principal elements, where the traditional thought on the structure selection can no longer be applied directly. Recent studies revealed that the valence electron concentration (VEC) is a dominant factor controlling the solid-solution structures of fcc and bcc in HEAs, on the premise that only solid solutions form and no intermetallic compounds form.[12] The average VEC in HEAs is defined as

$$\text{VEC} = \sum_i^n c_i (\text{VEC})_i \quad (4)$$

where $(\text{VEC})_i$ is the valence electron numbers for the ith atom.

Based on limited experiments on HEAs obtained so far, both the mixing enthalpy and atomic-size difference have been found to play dominant roles in controlling the phase stability in HEAs. Although the parameters of ΔH_{mix} and δ are more empirical in nature and the physical meaning of VEC is not well understood, these empirical parameters provide useful guidance for phase selection in HEAs.

PHASE SELECTION AT ELEVATED TEMPERATURES NEAR THE MELTING POINT

The phase stability of solid solutions, intermetallic compounds, and amorphous alloys has been discussed for HEAs.[10–14] Most previous discussions on the phase selection were based on the as-cast samples prepared with rapid solidification. Therefore, the phase selection discussed for as-cast samples is more suitable for the case of high temperatures caused by the sluggish diffusion effects in HEAs. Plenty of HEAs experiments indicate that the solid solutions in HEAs are favored in the region of $5\,\text{kJ/mol} \geq \Delta H_{\text{mix}} \geq -15\,\text{kJ/mol}$ and $\delta \leq 6.6\%$, as indicated in Fig. 1.[10,14] Beyond this region, intermetallic compounds have a chance to occur and meta-stable amorphous alloys can also appear following the fast quenching.

Solid Solutions

The tendency to form simple solid solutions is one of the main features for HEAs with equiatomic

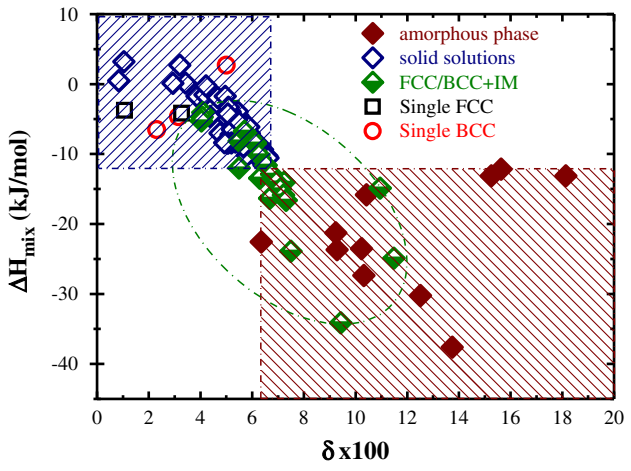

Fig. 1. The $\Delta H_{\text{mix}} - \delta$ plot delineating the phase selection in HEAs in the as-cast state. The oval zone is for mixed solid solutions, intermetallic compounds, and metallic glasses.[14]

compositions. Most solid-solution HEAs have fcc and bcc structures. Very recently, the possible formation of hexagonal close-packed (hcp) structure was addressed in Reference [18], and the potential hcp phase forming alloy systems were suggested. Up to now, only limited HEAs have found to be a single-phased solid solution, and most alloy systems essentially contain essentially mixed solid solutions. The search for single-phased solid-solution alloys has been discussed from theoretical considerations.[18] Experimentally, a single fcc structure is found in CoCrFeMnNi and its subsets of CoCrFeNi, CoFeMnNi, and CoCrMnNi.[19] Alloys with a single bcc structure include MoNbTaW,[20,21] MoNbTaWV,[20,21] and HfNbTaTiZr containing mainly refractory alloying elements.[22] Note that all these alloys are in a much narrow range of $\Delta H_{mix} > -7.5$ kJ/mol and $\delta < 4.5\%$, as shown in Fig. 1. The formation mechanism for single-phased solid solution is still not well understood. The mixing enthalpy and atomic-size difference only indicates the possibility of forming a solid solution, i.e., they are necessary but not sufficient requirements. The phase separation and intermetallic precipitation are the two factors hindering the formation of single-phased solid solution in HEAs. The single-phased solid solution can form in the systems without a strong short-range order CoCrFeNi.[23] In ab initio molecular dynamics simulations, the elements are distributed randomly in the liquid state of an HfNbTaTiZr alloy.[18] The diffusion constant in the liquid alloys is another factor affecting the formation of single-phased solid solutions. The Cu atom has the fastest diffusivity in the $CoCrCuFeNiAl_{1.3}$ alloy and positive mixing enthalpies with other elements, both of which enhance the segregation of Cu.[18]

Some HEAs contain multiple solid solutions, including fcc phases, mixed fcc/bcc phases, and bcc phases. In the CoCrCuFeNi alloy, there are two different fcc phases in the primary dendrite and interdendrite with different Cu concentrations.[24] In Al_xCoCrFeNi system, the mixed fcc/bcc phases appear at $0.4 < x < 0.8$ and the spinodal-decomposed two bcc phases appear at $x > 0.9$.[25] Statistic analyses of previous solid solutions forming in HEAs showed that the fcc phase is stable at a higher VEC (>7.8), bcc phase is stable at a lower VEC (<6.8), and mixed fcc and bcc phases appear in the intermediate range.[12] The mechanism of the VEC rule for the phase selection is not well understood. The first-principles calculations have been proven as a powerful tool for the phase selection of HEAs.[26] The relationship between the VEC and the Fermi level should be further evaluated[27] to reveal the mechanism for VEC rule to work efficiently in the phase selection of HEAs.

Intermetallic Compounds

Intermetallic compounds in HEAs have received much less attention compared with the solid solutions. Recently, μ, σ, χ, and Laves phases have been confirmed in well-annealed HEAs.[28,29] The formation of these topologically close-packed phases roots in the nature of alloying elements in HEAs. These intermetallic compounds appear in the binary and ternary phase diagrams, such as Co-Mo, Co-Ti, Fe-Ti, Fe-Cr, Ni-Al, Co-Mo-Fe, etc.[28] Most of these intermetallic compounds are composed of the elements in VIIB or VIIIB and VIIB and VIIIB in the Periodic Table. In HEAs, a large configurational entropy and small atomic-size difference are expected to suppress the formation of intermetallic compounds, such as in the CoCrFeNi alloy. Thus, intermetallic compounds appear only in the HEAs with quite negative $\Delta H_{mix} < -15$ kJ/mol and a large $\delta (> 6.6\%)$, as shown in Fig. 1. The formation of intermetallic compounds in HEAs usually decreases the ductility of alloys, but their contribution to the hardness and strength is certainly attractive. By properly designing the alloying compositions, the mechanical properties of HEAs can be significantly improved through dispersed intermetallic particles. Certainly, the formation and dispersion of intermetallic compounds in HEAs deserves more attention in the future development of HEAs with desirable mechanical properties.

Amorphous Alloys

The alloy compositions in certain HEAs are similar to those for bulk amorphous alloys, or better known as bulk metallic glasses (BMGs). The design principles for BMGs share three common factors with HEAs: element number, atomic-size difference, and mixing enthalpy. However, the requirements for BMGs are usually in the opposite direction as to those for solid solutions in HEAs. Most of previous BMGs have three or four elements, where the configurational entropy is in the medium range. Recent experiments found some metallic glasses with a high configurational entropy.[30–33] In the $\Delta H_{mix} - \delta$ plot, these high-entropy metallic glasses are randomly distributed[14,34] and the regions of metallic glasses and the intermetallic compounds are overlapping, indicating that they compete with each other during solidification, i.e., the competition between the short-range order and the long-range order.

It is worthy of noting an unexpected case of $Al_{0.5}$TiZrPdCuNi alloy during the search for high-entropy metallic glasses.[35] This alloy showed an amorphous phase in the melt-spun sample, while a bcc phase without intermetallic compounds is shown in the 1.5 mm as-cast samples. It seems that the metallic glass competes well with the solid solution phases, rather than intermetallic compounds, during solidification in this system. In this alloy, $\Delta H_{mix} = -46.7$ kJ/mol and $\delta = 8.8\%$, both of them are out of the conventional solid-solution region. The Al-free alloy TiZrPdCuNi is composed of intermetallic compounds, with $\Delta H_{mix} = -45.1$ kJ/mol and $\delta = 9.2\%$. The phase selection rules based on the configuration-entropy, mixing-enthalpy and atomic-size differences apparently

fails to work for this system. Further understanding into this exception is certainly required.

PHASE STABILITY WITHIN A CERTAIN TEMPERATURE RANGE

The phase selection in HEAs discussed in the previous section is based on as-cast samples under rapid solidification in copper molds. The thermal treatment of some as-cast samples of HEAs could induce the phase transformation. Although the sluggish diffusion effect in HEAs could retard the solid phase transformation,[36,37] the solid solutions in HEAs existing at high temperatures could be unstable as the temperature decreases because the contribution of the configurational entropy in the Gibbs free energy decreases. In some HEAs, intermetallic compounds precipitate out after a long-time annealing at intermediate temperatures.[36] Solid-solution forming HEAs, particularly fcc structured HEAs, generally have a good ductility, and they are most attractive for structure applications. Here, the stability of solid solutions in a certain temperature range will be emphasized. We will discuss the selection of equilibrium phases in HEAs based on available aging experiments data. The temperatures used for thermal treatments are usually in the range of $0.5 < T/T_m < 0.9$.

Homogenization and Aging

The solubility and phase stability are found to change substantially after homogenization treatments of many HEAs at high temperatures below their melting points. In $Al_xCoCrCuFeNi$ or $Al_xCoCrFeNi$ systems, the homogenization will reduce the composition range for fcc and bcc phases. After the homogenization of the $Al_xCoCrFeNi$ alloys at 1100°C, the single fcc solid solution was found to exist only at $x < 0.3$ in the homogenized condition, while the solubility of Al had extended to $x < 0.45$ in the as-cast condition.[38] This is because the solid solubility limit generally decreases as the temperature decreases. During the homogenization process, intermetallic compounds show up in some HEAs.[28] For example, after homogenization at 1000°C for 3 days, the μ phase appears in the CoFeMnMoNi alloy, and both χ and Laves phases were precipitated out in the CrFeMnNiTi alloy. The σ phase is formed in some systems containing Cr and V, and the bcc phase may also transform directly to the σ phase without a composition change after aging at 700°C.[29] The intermetallic compounds were also observed in the in $Al_xCoCrFeNi$ systems at $x > 0.3$; however, the volume fraction of intermetallic compounds is very small at $x > 0.88$ after homogenization at 1100°C.[38]

Thermomechanical Treatment

The increased strain energy and induced defects after cold working greatly increase the driving force for the solid-state phase transformation. The annealing of cold-worked samples results in the formation of stable phases more quickly than that without mechanical treatment. Among HEAs, the annealing effect has been investigated extensively in the $Al_{0.5}CoCrCuFeNi$ alloy.[36,39] In this system, the samples were cold worked before annealing. The fcc, bcc, and σ phase coexist in the samples after annealing around 700°C. At 900°C, the annealed samples contain the fcc and bcc phases. Above 1100°C, the samples consist of only two fcc phases, the same as that in the as-cast samples. In the single-phased fcc alloys of CoCrFeNi, CoFeNi, and CoCrNi, the samples with annealing of 1 h after the cold rolling did not show any phase transformation at temperatures from 300°C to 1000°C.[19] The result of a longer annealing is not reported yet. It is possible to form intermetallic precipitations in these alloys after long-term annealing because the formation of intermetallic phases and bcc phases in these alloys has been revealed by phase diagram calculations.[19]

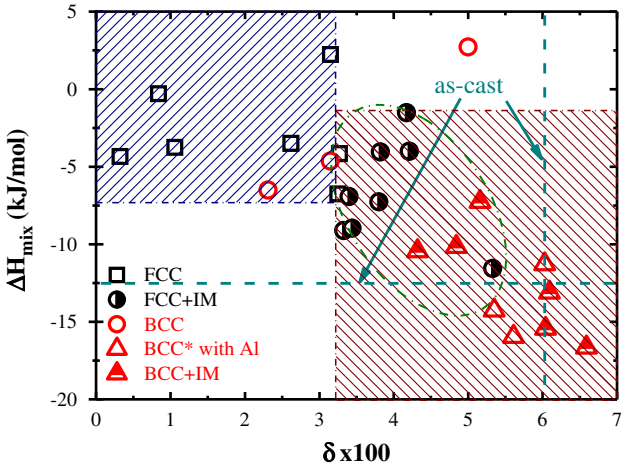

Fig. 2. The $\Delta H_{mix} - \delta$ plot delineating the phase selection after thermal treatments in the temperature range ($0.5 < T/T_m < 0.9$). The oval zone includes Al-added alloys. The asterisk denotes that the intermetallic phases in these alloy systems need to be checked further.

Criteria for the Equilibrium Phase Selection

Figure 2 is a plot of $\Delta H_{mix} - \delta$ to show the phase selection of HEAs in a temperature range of $0.5 < T/T_m < 0.9$ based on the available data. These data are also listed in Table I together with their references. This plot clearly shows that the region for the solid solutions shrinks significantly after thermal treatments, as indicated by a much smaller region compared with the region of solid solutions in the as-cast state. The plot shows that the region containing the fcc and bcc solid solutions is stable at $\Delta H_{mix} > -7.5$ kJ/mol and $\delta < 3.3$, which is much smaller than that of the as-cast state as indicated by the dashed line in Fig. 2. It confirms that the configurational entropy appears to play a less important role at lower temperatures. Some intermetallic compounds appear at $\Delta H_{mix} < -7.5$ kJ/mol and $\delta > 3.3$. However, the Al-added bcc solid

solutions are not what is expected. In these annealed samples, the intermetallic precipitates can be observed by the scanning electron microscopy (SEM) and transmission electron microscopy (TEM), but they were not revealed from the x-ray diffraction (XRD). Note that most of phases in Fig. 2 were identified only from the XRD; thus, the intermetallic precipitates in the asterisk-marked alloys need to be further checked. In these alloys, usually the spinodal-decomposed bcc phases are more stable and the volume fraction of intermetallic compounds is very small. Perhaps additional work using TEM, three-dimensional atomic probe, or neutron-scattering studies is required to provide more information on the phase formation in these Al-added bcc HEAs. Also, it is expected that these sophisticated microanalyses may provide a clue for the formation of the bcc phase in $Al_{0.5}TiZrPdCuNi$ with $\Delta H_{mix} = -46.7\,kJ.mol^{-1}$ and $\delta = 8.8$, largely exceeding the previous established phase selection rule.[34]

Figure 3 shows the VEC plot with the data obtained from thermal treatments. This plot reveals that the intermetallic compounds appear within the range of $7.8 > VEC > 6.0$, and the fcc and bcc phases are still stable for $VEC > 7.8$ and $VEC < 6.0$, respectively. There is a little change of the fcc region, but the bcc region becomes much smaller after annealing. The annealing induces the formation of intermetallic compounds in the previous mixed fcc and bcc region for the as-cast state. The simple VEC rule is still effective in predicting the phase selection within certain temperature ranges. It was also found

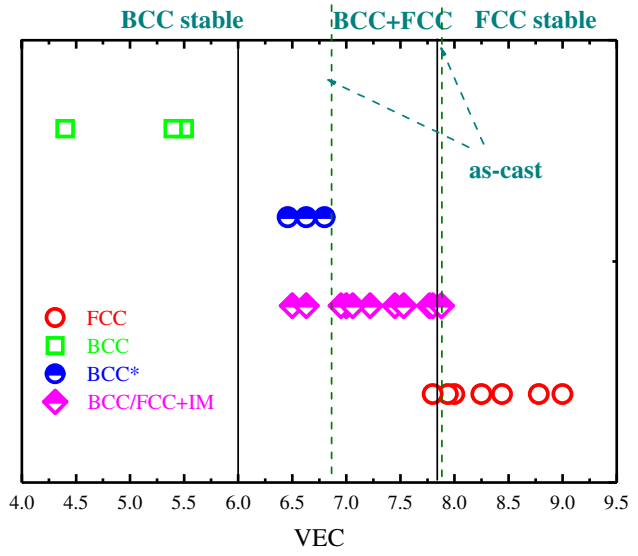

Fig. 3. Relationship between the VEC and the phase stability after thermal treatments in the temperature range of $0.5 < T/T_m < 0.9$. The asterisk denotes that the intermetallic compounds in these alloy systems need to be checked further.

Table I. The ΔH_{mix}, δ, VEC, and Phases after Thermal Treatment at Finite Temperature in some HEAs, Which are also Plotted in Figs. 2 and 3

Material	$\delta \times 100$	ΔH_{mix}(kJ/mol)	VEC	Phases	References
CoCrFeMnNi	3.27	–4.16	8	fcc	28
CoCrFeNi	1.06	–3.75	8.25	fcc	19
$CoCrFeNiAl_{0.25}$	3.25	–6.75	7.94	fcc	38
$CoCr_2FeNi$	0.3215	–4.34	7.8	fcc	29
$Co_{1.5}Cr_{0.5}FeMn_{0.5}Ni$	2.6192	–3.5	8.44	fcc	29
FeCoCrMnCu	3.15	2.24	9	fcc	28
$FeCoNiCrCu_{0.5}$	0.84	–0.30	8.78	fcc	40
WNbMoTa	2.31	–6.5	5.5	bcc	21
WNbMoTaV	3.15	–4.64	5.4	bcc	21
TaNbHfZrTi	4.99	2.72	4.4	bcc	22
$CoCrFeNiAl_{0.3}$	3.8	–7.26	7.88	fcc + ordered phase	41
$CoCrFeNiAl_{1.17}$	6.094	–13.1	7.06	bcc + ordered phase	38
$CoCrFeNiAl_2$	6.04	–15.44	6.5	bcc + ordered phase	38
$Co_{0.5}Cr_{0.5}Fe_{0.5}NiAlMnV$	5.35	–14.26	6.63	bcc*	29
$Co_{0.5}Cr_{0.5}Fe_{0.5}NiAlMnV_{0.5}$	5.61	–15.96	6.8	bcc*	29
$CrMnFe_{1.5}Ni_{0.5}Al_{1.2}$	6.03	–11.28	6.46	bcc*	29
$CoCrFeNiTi_{0.5}$	5.33	–11.56	7.77	fcc + IM	42
$CoCrFeNiCuAl_{0.5}$	4.17	–1.52	7.45	fcc + bcc + IM	36
$Co_{0.5}CrFeMn_{1.5}Ni$	3.73	–4.04	7.8	fcc + IM	29
$CrMnFe_{1.5}Ni_{0.5}Al_{0.5}$	5.16	–7.26	7	bcc + IM	29
$CoCr_2FeNiAl_{0.3}$	3.4	–6.92	7.53	fcc + bcc + IM	29
$CoCrFeNiAl_{0.4}MnV$	4.32	–10.43	7.22	IM#	29
$Co_{1.5}Cr_2Fe_{1.5}NiAlMn_2V$	4.84	–10.15	6.95	IM#	29
FeCoNiMnV	3.44	–8.96	7.8	fcc + IM	28
FeCoNiMnMo	4.21	–4	8	fcc + IM	28
FeNiCrMnTi	6.59	–16.64	7	fcc + bcc + IM	28
NiCoCrMnV	3.33	–9.12	7.6	fcc + IM	28

IM intermetallics, * denotes the phases in the alloys, # denotes there are only IM in the alloys.

that the σ phase, as an electron intermetallic compound, is favored in the region of $7.84 > \text{VEC} > 6.88$ in HEAs.[29] These results are similar to the VEC rule of solid solutions in the as-cast state but with a different critical value.[12]

Experimental results from thermal treatments of HEAs indicate that the high configurational entropy alone is insufficient in suppressing the formation of intermetallic compounds, especially at lower temperatures. The configurational entropy for equiatomic HEAs with five elements is 13.38 kJ/mol. For some metallic pairs, the mixing enthalpy is quite negative, such as $\Delta H^{\text{mix}}_{\text{Ni,Ti}} = -35$ kJ/mol. As a result, the configurational entropy is insufficient to suppress all intermetallic pairs in HEAs, especially after thermal or thermomechanical treatments.

CONCLUSION

The recent progress in the phase selection of HEAs is summarized and analyzed based on the mixing enthalpy, atomic-size difference, and valence-electron concentration. Although the high configurational entropy supposedly favors the solid solutions, intermetallic compounds are found to exist in many HEAs. In addition to the atomic size effect, the enthalpy of mixing among alloying elements also plays an important role in the phase selection of HEAs. The mixing enthalpy ΔH_{mix} and atomic-size difference δ both strongly affect the phase selection. In the high temperature near the melting point, the solid solutions are favorably formed in the region of $5\,\text{kJ/mol} \geq \Delta H_{\text{mix}} \geq -15\,\text{kJ/mol}$ and $\delta \leq 6.6\%$, and the stable intermetallic compounds and even metastable metallic glasses appear at $\Delta H_{\text{mix}} < -15\,\text{kJ/mol}$ and $\delta > 6.6\%$ in certain as-cast samples. The VEC can be used to verify the solid solution structure: fcc at $\text{VEC} > 7.84$, bcc at $\text{VEC} < 6.87$, and mixed fcc and bcc in the range between them. At lower temperatures within $0.5 < T/T_{\text{m}} < 0.9$, the equilibrium phase selection criteria change due to the reduced configurational entropy effect. Most of the solid solutions shrinks to $\Delta H_{\text{mix}} \geq -7.5\,\text{kJ/mol}$ and $\delta < 3.3\%$ after thermal or thermomechanical treatments. The VEC plot shows that the intermetallic compounds appear in the medium range of VEC, and the fcc and bcc solid solution phases are more stable at $\text{VEC} > 7.8$ and $\text{VEC} < 6.0$, respectively.

ACKNOWLEDGEMENTS

This research is supported by the Research Grant Council (RGC), the Hong Kong Government, through the General Research Fund (GRF) under the project numbers CityU/521411. Zhijun Wang is supported by the GRF Grant, the Hong Kong scholar program, and the National Science Foundation for Post-doctoral Scientists of China under the project number 2013M542385.

REFERENCES

1. J.W. Yeh, S.K. Chen, S.J. Lin, J.Y. Gan, T.S. Chin, T.T. Shun, C.H. Tsau, and S.Y. Chang, *Adv. Eng. Mater.* 6, 299 (2004).
2. B. Cantor, I.T.H. Chang, P. Knight, and A.J.B. Vincent, *Mater. Sci. Eng. A* 375, 213 (2004).
3. J.W. Yeh, *Annal. Chim. Sci. Des.* 31, 633 (2006).
4. Y. Zhang, X. Yang, and P.K. Liaw, *JOM* 64, 830 (2012).
5. J.W. Yeh, *JOM* 65, 1759 (2013).
6. Y. Zhang, T.T. Zuo, Z. Tang, M.C. Gao, K.A. Dahmen, P.K. Liaw, and Z.P. Lu, *Progr. Mater. Sci.* 61, 1 (2014).
7. C.J. Tong, Y.L. Chen, S.K. Chen, J.W. Yeh, T.T. Shun, C.H. Tsau, S.J. Lin, and S.Y. Chang, *Metall. Mater. Trans. A* 36, 881 (2005).
8. C.Y. Hsu, C.C. Juan, S.T. Chen, T.S. Sheu, J.W. Yeh, and S.K. Chen, *JOM* 65, 1829 (2013).
9. F. Zhang, C. Zhang, S.L. Chen, J. Zhu, W.S. Cao, and U.R. Kattner, *CALPHAD* 45, 1 (2014).
10. Y. Zhang, Y.J. Zhou, J.P. Lin, G.L. Chen, and P.K. Liaw, *Adv. Eng. Mater.* 10, 534 (2008).
11. S. Guo and C.T. Liu, *Prog. Nat. Sci.* 21, 433 (2011).
12. S. Guo, C. Ng, J. Lu, and C.T. Liu, *J. Appl. Phys.* 109, 103505 (2011).
13. X. Yang and Y. Zhang, *Mater. Chem. Phys.* 132, 233 (2012).
14. S. Guo, Q. Hu, C. Ng, and C.T. Liu, *Intermetallics* 41, 96 (2013).
15. W.R. Wang, W.L. Wang, and J.W. Jeh, *J. Alloy Compd.* 589, 143 (2014).
16. A. Gali and E.P. George, *Intermetallics* 39, 74 (2013).
17. W. Hume-Rothery and G.V. Raynor, *The Structure of Metals and Alloys*, 5th ed. (London, UK: Institute of Metals, 1969).
18. M.C. Gao and D.E. Alman, *Entropy* 15, 4504 (2013).
19. Z. Wu, H. Bei, F. Otto, G.M. Pharr, and E.P. George, *Intermetallics* 46, 131 (2014).
20. O.N. Senkov, G.B. Wilks, D.B. Miracle, C.P. Chuang, and P.K. Liaw, *Intermetallics* 18, 1758 (2010).
21. O.N. Senkov, G.B. Wilks, J.M. Scott, and D.B. Miracle, *Intermetallics* 19, 698 (2011).
22. O.N. Senkov, J.M. Scott, S.V. Senkova, D.B. Miracle, and C.F. Woodward, *J. Alloys Compd.* 509, 6043 (2011).
23. M.S. Lucas, G.B. Wilks, L. Mauger, J.A. Munoz, O.N. Senkov, E. Michel, J. Horwath, S.L. Semiatin, M.B. Stone, D.L. Abernathy, and E. Karapetrova, *Appl. Phys. Lett.* 100, 251907 (2012).
24. Y.J. Hsu, W.C. Chiang, and J.K. Wu, *Mater. Chem. Phys.* 92, 112 (2005).
25. W.R. Wang, W.L. Wang, S.C. Wang, Y.C. Tsai, C.H. Lai, and J.W. Yeh, *Intermetallics* 26, 44 (2012).
26. F. Tian, L. Delczeg, N. Chen, L.K. Varga, J. Shen, and L. Vitos, *Phys. Rev. B* 88, 085128 (2013).
27. C.T. Liu, *Inter. Met. Rev.* 29, 168 (1984).
28. F. Otto, Y. Yang, H. Bei, and E.P. George, *Acta Mater.* 61, 2628 (2013).
29. M.H. Tsai, K.Y. Tsai, C.W. Tsai, C. Lee, C.C. Juan, and J.W. Yeh, *Mater. Res. Lett.* 1, 207 (2013).
30. H.Y. Ding, K.F. Yao, and J. Non-Cryst, *Solids* 364, 9 (2013).
31. X.Q. Gao, K. Zhao, H.B. Ke, W.H. Wang, H.Y. Bai, and J. Non-Cryst, *Solids* 357, 3557 (2011).
32. A. Takeuchi, N. Chen, T. Wada, Y. Yokoyama, H. Kato, A. Inoue, and J.W. Yeh, *Intermetallics* 19, 1546 (2011).
33. H.F. Lia, X.H. Xie, K. Zhao, Y.B. Wang, Y.F. Zhenga, W.H. Wang, and L. Qin, *Acta Biomater.* 9, 8561 (2013).
34. A. Takeuchi, K. Amiya, T. Wada, K. Yubuta, W. Zhang, and A. Makino, *Entropy* 15, 3810 (2013).
35. A. Takeuchi, J.Q. Wang, N. Chen, W. Zhang, Y. Yokoyama, K. Yubuta, and S.L. Zhu, *Mater. Trans.* 54, 776 (2013).
36. C. Ng, S. Guo, J. Luan, S. Shi, and C.T. Liu, *Intermetallics* 31, 165 (2012).

37. K.Y. Tsai, M.H. Tsai, and J.W. Yeh, *Acta Mater.* 61, 4887 (2013).
38. Y.F. Kao, T.J. Chen, S.K. Chen, and J.W. Yeh, *J. Alloy. Compd.* 488, 57 (2009).
39. C.W. Tsai, Y.L. Chen, M.H. Tsai, J.W. Yeh, T.T. Shun, and S.K. Chen, *J. Alloys Compd.* 486, 427 (2009).
40. C.M. Lin, H.L. Tsai, and H.Y. Bor, *Intermetallics* 18, 1244 (2010).
41. T.T. Shun and Y.C. Du, *J. Alloy. Compd.* 479, 157 (2009).
42. L. Jiang, Y. Lu, Y. Dong, T. Wang, Z. Cao, and T. Li, *Intermetallics* 44, 37 (2014).